ChemComm

Accepted Manuscript

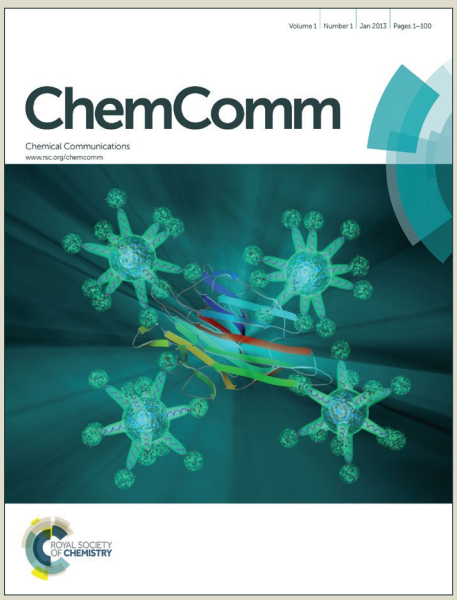

ROYAL SOCIETY OF CHEMISTRY

www.rsc.org/chemcomm

Journal Name

COMMUNICATION

Energy gap engineering of polymeric carbon nitride Nanosheets for matching with $NaYF_4$:Yb,Tm: enhanced visible-near infrared photocatalytic activity

Received 00th January 20xx,
Accepted 00th January 20xx

DOI: 10.1039/x0xx00000x

www.rsc.org/

Xuefeng Li,[a] Hao Ren,[c] Zhijuan Zou,[b] Jiaojiao Sun,[a] Jingyu Wang*[b] and Zhihong Liu*[a]

Molecularly grafted carbon nitride (CN) nanosheets, well matching the emission energy of upconversion phosphors (UCPs), were acquired for the first time. As a result of energy gap engineering, the assembled composites successfully realized the full use of visible-NIR light and afforded much higher activity than CN- or UCPs-based photocatalysts ever reported.

Polymeric carbon nitride (CN) semiconductor with a graphite-like structure, usually called Liebig's melon or g-C_3N_4, has gained increasing interest as a new class of catalyst possessing unique structural and electronic properties.[1-4] CN and its derivatives have shown promising prospect in photocatalysis owing to some notable merits, such as the abundant and low-cost nitrogen-rich precursors, low toxicity, high thermal and chemical stability, and especially the tunable bandgap.[5] Nevertheless, bulk CN is still subject to several restrictions in practical applications, including the limited photoresponsive range, low specific surface area,[6] and high recombination rate of photogenerated electron(e^-)-hole(h^+) pairs,[7] which lead to the insufficient use of solar energy and impaired catalytic efficiency.

Because of its layered structure analogous to that of graphite,[8] bulk CN has recently been successfully exfoliated into CN nanosheets (CN-NSs) consisting of few atomic layers.[9-12] Like graphene oxide, the improved water dispersibility by exfoliation is favorable for anchoring on other materials when constructing composite structures.[13] Moreover, the resulting 2D CN structure gives rise to both increased mobility of charge carriers and larger specific surface area,[9-12] which partly circumvents the deficiencies of bulk material. Unfortunately, this is at the cost of utilizable light range in the previous literature, since the exfoliated CN-NSs bring out a blue shift of the absorption edge presumably due to the decrease of conjugation length and the strong quantum confinement effect.[9-12] Therefore, it still remains a great challenge for the effective use of CN as a photocatalyst.

Herein, we propose a strategy to improve the activity of CN by integrating a molecular grafting approach with a liquid phase assembly process. Our design involves two consecutive steps (Scheme 1): 1) Copolymerization of carbon nitride precursor with an organic monomer 2-aminobenzonitrile followed by an exfoliation process, so as to obtain the merits of 2D structure and to reduce the energy gap (bathochromic shift to visible light range); 2) Coupling the doped CN-NSs with UCPs, which convert NIR light to visible light through the anti-Stokes photoluminescence,[14,15] thus making use of NIR light in photocatalysis. The as-obtained composites (UCPs/CNX_n-NSs, C is 2-aminobenzonitrile and n is the doping amount) behave as more efficient visible-NIR photocatalysts than previous CN- or UCP-based materials. This strategy opens up a valuable way to design energy-matched acceptors for UCPs and achieve sufficient utilization of solar energy.

At the first step of molecular grafting, we investigated the effects of both copolymerization and exfoliation on the physicochemical and photocatalytic properties of CN. To this end, we prepared four materials including two bulk-phase CN(CN and $CNX_{0.1}$) and two exfoliated nanosheets (CN-NSs and $CNX_{0.1}$-NSs). The crystal structures of the materials were

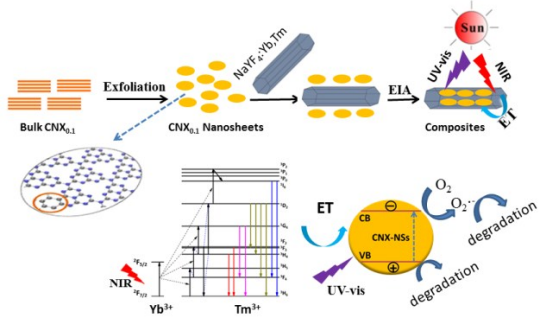

Scheme 1 The fabrication process of UCPs/$CNX_{0.1}$-NSs and photocatalytic mechanism of UCPs/$CNX_{0.1}$-NSs under solar light.

[a] Key Laboratory of Analytical Chemistry for Biology and Medicine (Ministry of Education), College of Chemistry and Molecular Sciences, Wuhan University, Wuhan 430072, China. Email: zhhliu@whu.edu.cn.
[b] Key Laboratory of Large-Format Battery Materials and System (Ministry of Education), School of Chemistry and Chemical Engineering, Huazhong University of Science and Technology, Wuhan 430074, China. Email: jingyu.wang@163.com.
[c] Center for Bioengineering and Biotechnology, China University of Petroleum (Huadong), Qingdao 266580, China.

Electronic Supplementary Information (ESI) available: [Experimental details, further characterization, and calculation results]. See DOI: 10.1039/x0xx00000x

examined by X-ray diffraction (XRD). As seen in Fig. 1a, both $CNX_{0.1}$ and CN show a dominant peak at 27° originating from the (002) interlayer diffraction of graphite-like structures and a small peak at 13° attributable to the (100) in-plane repeat units of triazine.[1] The slight weakening of characteristic peaks in $CNX_{0.1}$ suggests that copolymerization blocks the periodic linkage of triazine units by introducing phenylene groups into CN networks.[16] For exfoliated NSs, although some monolayer NSs are reported to form agglomerates during the preparation of powders for XRD measurement,[11] the patterns of CN-NSs and $CNX_{0.1}$-NSs still exhibit sharp decrease in the (002) diffraction, indicating that the interlayer stacking of CN is significantly weakened by exfoliation. Meanwhile, the disappearance of (100) in-plane diffraction signal of the nanosheets can be ascribed to the decreased planar size of the CN layers.[17,18] This can also be confirmed by transmission electron microscopy (TEM) and atomic force microscopic (AFM) observations. The randomly measured NSs display planar size of 60~120 nm and the thickness of 0.6~4 nm (about 2-10 C–N layers) (Fig. 1b-e). The FTIR spectra (Fig. S1, ESI†) show that all the four materials display the characteristic absorption bands of CN networks, which means the copolymerization with 2-aminobenzonitrile and exfoliation do not alter the core chemical skeleton of CN too much because of the low doping amount.[16] The chemical states and compositions of $CNX_{0.1}$ and $CNX_{0.1}$-NSs were investigated by X-ray photoelectron spectroscopy (XPS). There is no obvious shift of binding energy of C 1s and N 1s core electrons (Fig. S2, ESI†), suggesting that the local chemical environments of both C and N atoms in the nanosheets are conserved as in the bulk materials. It is also revealed by the survey spectra that the amount of O adsorbed or bonded on $CNX_{0.1}$-NSs is higher than that on $CNX_{0.1}$ (Table S1, ESI†). This can be explained by the oxidization of bulk phase during exfoliation.

We then studied the effect of copolymerization and exfoliation on the intrinsic electronic structure of CN. The absorption edge of ultrathin CN-NSs shows a blue shift from 457 nm to 429 nm in comparison with bulk CN, corresponding to an increase in the energy gap from 2.71 eV to 2.89 eV (Fig. 2a), which is in consistence with the literature.[9-12] The

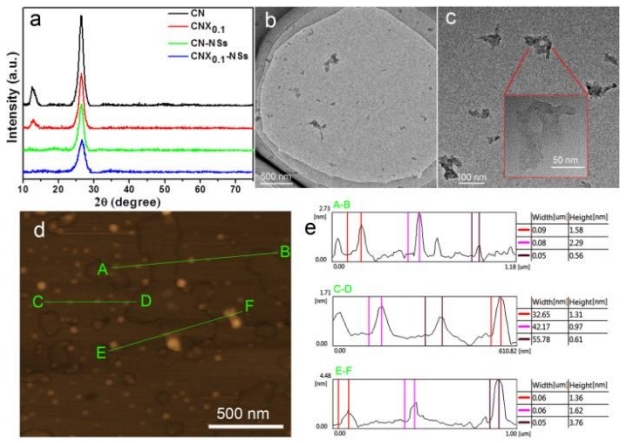

Fig. 1 (a) XRD patterns of CN, $CNX_{0.1}$, CN-NSs, and $CNX_{0.1}$-NSs. TEM (b, c) and AFM (d) images of exfoliated $CNX_{0.1}$-NSs. (e) The corresponding height curves determined along the lines in (d).

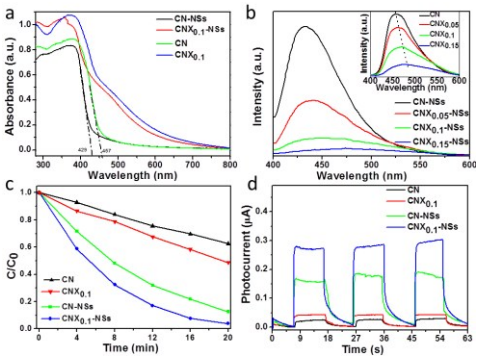

Fig. 2 (a) UV–Vis diffuse reflectance spectra (DRS). (b) PL spectra under 387 nm excitation. (c) Photocatalytic decomposition of rhodamine B (RhB) and (d) Photocurrent response under visible light illumination (λ >400 nm).

incorporation of phenylene groups into CN networks, as expected, brings forth a remarkable red shift of the optical absorption in both bulk $CNX_{0.1}$ and $CNX_{0.1}$-NSs (Fig. 2a). To further inspect the effect of the 2-aminobenzonitrile content on the photophysics, we prepared materials with varying doping amounts, i.e., n=0.05, 0.1, and 0.15, respectively. For both bulk materials (Fig. S3a, ESI†) and nanosheets (Fig. S3b, ESI†), the absorption in the visible region is obviously enhanced along with X content. These results have vividly validated the function of 2-aminobenzonitrile doping in the adjustment of the energy gap of CN. Further evidences can also be found in the photoluminescence (PL) spectra of these materials. The PL emission of ultrathin CN-NSs also shows a blue shift of ~26 nm compared with bulk CN. Similarly, the PL peaks of both the bulk-phase and the nanosheet materials shift towards longer wavelength after the copolymerization of CN with 2-aminobenzonitrile (Fig. 2b). Moreover, the extent of the red shift of PL emission also increases with the X content. The results are also supported by theoretical calculations (Fig. S13-19, Table S3-4, ESI†). The self-consistent density functional tight-binding (SCC-DFTB) and semiempirical ZINDO methods present the following results: (1) copolymerization leads to remarkable red shift of the absorption edge, suggesting that the energy gap is narrowed due to the extension of π-conjugation system; (2) exfoliation process causes the shift to the opposite direction because of the strong quantum confinement effect; (3) the influence of exfoliation is less significant than that of copolymerization, especially for phenylene doped CN systems. From our experiments and calculations, it is clear that exfoliating bulk CN into ultrathin nanosheets is unfavorable for visible light utilization because of the increased energy gap; yet it is essential for separating charge carriers and enlarging specific surface area.[11] Fortunately, such a conflict can be circumvented by the incorporation of phenylene groups which effectively reduce the energy gap. Therefore, it is still possible for ultrathin CNX NSs to utilize a wide range of visible light in photocatalysis.

With the engineering of energy gap verified, we then examined the photocatalytic activities of the materials by degrading rhodamine B (RhB) under visible light irradiation. In accordance with the above physical properties, the catalytic activities of X doped materials are significantly higher than

those of their undoped contrasts, as shown in Fig. 2c. This confirms the significance of adjusting the energy gap and light absorption. The influence of doping amount on the activity (Fig. S4, ESI†) suggests that a low degree of copolymerization is optimal to improve the catalytic activity; while excessive dopant is likely to spoil the electronic structure and impair photocatalysis.[16,19] Another meaningful result is that the activity of CN-NSs is still better than that of CN although it absorbs less visible light, which undoubtedly can be attributed to the more efficient separation of charge carriers and the larger specific surface area.

The electrochemical and photoelectrochemical properties of the materials were measured by electrochemical impedance spectroscopy (EIS) and photocurrent, respectively. Nyquist plots of $CNX_{0.1}$ and CN-NSs both display decreased semicircles compared to CN (Fig. S5, ESI†), indicating an improved electronic conductivity in the non-photoexcited state. $CNX_{0.1}$-NSs possess the lowest value of interfacial charge transfer resistance, suggesting the most efficient charge transfer across the electrode/electrolyte interface. It is recognized that the level of photocurrent generally reflects the efficiency of charge transfer. Fig. 2d shows an enhancement in the photocurrent signals of $CNX_{0.1}$ and CN-NSs over CN by a factor of 1.7 and 6.6, respectively. This indicates that the extension of π-conjugation system and the decrease of size in one dimension both facilitate the charge transfer and separation. As predicted, $CNX_{0.1}$-NSs possesses much higher photocurrent and photocatalytic activity than CN, $CNX_{0.1}$ and CN-NSs, which well demonstrates the synergistic effect of the two factors, i.e., exfoliation and doping that both reduce the recombination of photoinduced e^--h^+ pairs.

After achieving the improvement of catalytic activity of CN with the ability to use visible light, we further moved on to the second step of our design, in which the doped nanosheets were coupled with UCPs to utilize the NIR light for photocatalysis. There have been reports on the combination of UCPs with some inorganic semiconductors (SCs), such as TiO_2, ZnO, etc.[20-23] However, the efficiencies of utilizing NIR light of those complexes are unsatisfying because of the inflexible band structure of those inorganic SCs as well as the hindered excitation of UCPs due to serious light scattering by SCs. Apparently, the readily tunable energy gap and highly transparent morphology of CN are likely to make better use of the upconverted energy from NIR light. In view of the light absorption of the doped CN nanosheets, we selected $NaYF_4$:Yb,Tm with strong emissions at visible region as the upconversion material.[14,15] The $NaYF_4$:Yb,Tm microrods were synthesized via a modified hydrothermal method.[24] Scanning electron microscopy (SEM) image shows the uniform size of $NaYF_4$:Yb,Tm rods (~1.3 μm in length and ~240 nm in diameter) (Fig. 3a). The microrods were coated with polyacrylic acid (PAA) molecules on the surface, which can be characterized by FTIR (Fig. S6, ESI†). Zeta potential measurements show that the PAA coated UCPs colloids are negatively charged (-6.5 mV, Fig. S7, ESI†).[25] Meanwhile, the zeta potential of $CNX_{0.1}$-NSs colloids is +23.2 mV in neutral aqueous dispersion. The complex UCPs/$CNX_{0.1}$-NSs was then prepared with liquid-phase solvent evaporation induced assembly (EIA) (Scheme 1). During the process, the water soluble $CNX_{0.1}$-NSs assemble spontaneously on the surface of oppositely charged UCPs microrods through electrostatic attraction to minimize the total interfacial energy. The XRD patterns confirm the coexistence of CN networks and hexagonal phase $NaYF_4$ with high crystallinity in the complex (Fig. S8, ESI†). The SEM and TEM images (Fig. 3b and c) indicate that UCPs rods are decorated with ultrathin $CNX_{0.1}$-NSs on the surface after EIA. High-resolution TEM (HRTEM) shows that some CNX-NSs form a thin layer with a thickness of several nanometers covering UCPs rods (Fig. 3d), resulting from a curling and regrowth process driven by solvent evaporation.[26] The surface element composition measured by energy-dispersive X-ray spectroscopy (EDX) shows more evidence of the CN-UCPs coupling (Fig. S9, ESI†).

We then looked into the energy match between the emission of UCPs and the absorption of CN nanosheets, which is a decisive factor of the energy-transfer efficiency. The photoluminescence of UCPs, UCPs/CN-NSs and UCPs/CN $X_{0.1}$-NSs under 980-nm excitation were measured and compared (Fig. 4a), in which the concentration of UCPs was fixed. $NaYF_4$:Yb,Tm has several emission bands in both the UV region (291, 348, and 361 nm) and visible region (453 and 478 nm), corresponding to $^1I_6 \rightarrow {}^3H_6$, $^1I_6 \rightarrow {}^3F_4$, $^1D_2 \rightarrow {}^3H_6$, $^1D_2 \rightarrow {}^3F_4$, $^1G_4 \rightarrow {}^3H_6$ transitions of Tm^{3+} ions, respectively.[20] As shown in Fig. 4a, the coupling with undoped CN-NSs results in an obvious decrease in the emission of UV region and negligible changes in the emission of visible region. This can be explained with the fact that the absorption of CN-NSs covers only the emission of UCPs in UV region (the blue dashed line in Fig. 4a). On the other side, this phenomenon also implies that the CN-NSs with several-atoms thickness do not weaken the light intensity arriving at the UCPs surface, which usually occurs in most inorganic semiconductors-UCPs composites. In the case of $CNX_{0.1}$-NSs that absorb in the whole UV-Vis range and overlap with all the emission bands of $NaYF_4$:Yb,Tm, the emission of UCPs in both the UV and Vis regions are reduced remarkably, suggesting the efficient energy transfer from UCPs to $CNX_{0.1}$-NSs in the composite.

Ultimately, we evaluated the photocatalytic performance of the composite materials by detecting the degradation of RhB. Control experiments were conducted to preclude the

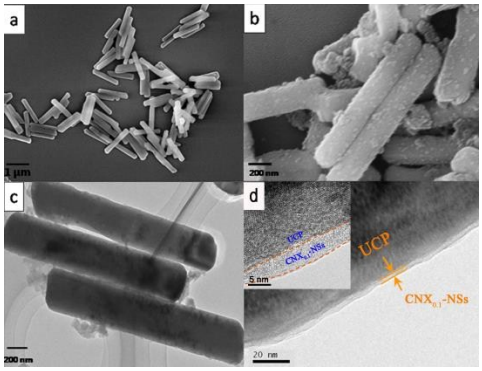

Fig. 3 SEM images of $NaYF_4$:Yb,Tm (a) and UCPs/$CNX_{0.1}$-NSs (b); (c) TEM and (d) HRTEM images of UCPs/$CNX_{0.1}$-NSs. The inset in d is the further magnification image.

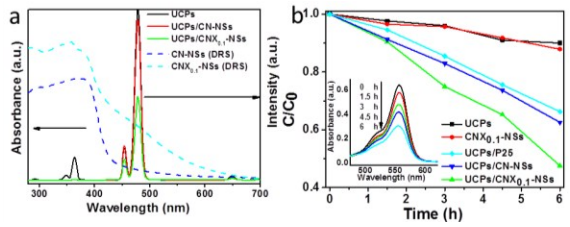

Fig. 4 (a) Luminescence spectra of UCPs, UCPs/CN-NSs, and UCPs/$CNX_{0.1}$-NSs under 980 nm excitation. (b) Photocatalytic degradation rates of RhB dye under 980 nm irradiation. The inset is time-dependent absorption spectra of RhB for UCPs/$CNX_{0.1}$-NSs.

influence of thermolysis or photolysis of the dye. The relative concentrations (C/C_0) were recorded with respect to the changes of absorbance of RhB at 554 nm (Fig. 4b). In the presence of UCP/$CNX_{0.1}$-NSs, the C/C_0 value of RhB decreases gradually under NIR irradiation. After 6 h, up to 52.4% of the dye was decomposed. While in other two control groups using UCPs or $CNX_{0.1}$-NSs alone as the catalyst, the decomposition of RhB was about 10% after NIR irradiation for 6 h. The results verify that the degradation of dye is attributed mainly to the photocatalytic activity of UCPs/$CNX_{0.1}$-NSs but little to thermolysis or photolysis. As an energy acceptor for UCPs, $CNX_{0.1}$-NSs are superior to undoped CN-NSs (Fig. 4b), as a result of the better energy match with UCPs. We further found that the photocatalytic activity of the composite was dependent on the mass ratio between UCPs and $CNX_{0.1}$-NSs (Fig. S10, ESI†). The optimum was achieved with UCPs:$CNX_{0.1}$-NSs = 1.5:1, which was compared with the published results in Table S2. The RhB degradation rate by UCPs/$CNX_{0.1}$-NSs under 980 nm in this work is about 1.5 times of that by Er^{3+} doped CN under red light irradiation.[27] In another degradation experiment under full range (visible-NIR light, Xe lamp with 400 nm filter) irradiation, the UCPs/$CNX_{0.1}$-NSs composite also showed a higher activity than UCPs/CN-NSs and UCPs/TiO_2 composites (Fig. S11, ESI†). The energy-transfer based photocatalysis mechanism is depicted in Scheme 1, in which $CNX_{0.1}$-NSs yield electrons and holes. The h^+ is capable of oxidizing RhB directly, and e^- can be trapped by adsorbed O_2 to produce superoxide radicals. The predominant contribution of h^+ and superoxide radicals to the photocatalytic reaction was confirmed by the scavenger test (Fig. S12, ESI†).

In conclusion, the molecularly grafted CN is exfoliated into ultrathin nanosheets and then successfully assembled on the surface of UCPs microrods. Compared with undoped bulk CN, the copolymerization extends the π-conjugation of CN network and reduces the gap energy. The engineered CN nanosheets possess extended light absorption, improved charge-carrier separation and enlarged surface area. Further assembly with UCPs makes $CNX_{0.1}$-NSs excitable by NIR light via the energy transfer from UCPs, owing to the ingenious gap-energy match. The UCPs/$CNX_{0.1}$-NSs composite exhibits so far the highest visible-NIR photocatalytic activity among all CN- or UCPs-based photocatalysts. Overall, the strategy presents new insights to design energy matched candidates for sufficient utilization of solar spectrum with diverse applications.

This work is financially supported by the National Natural Science Foundation of China (21575109, 21571071, 21375098) and the Natural Science Foundation of Hubei Province of China (2015CFB313).

Notes and references

1 X. C. Wang, K. Maeda, A. Thomas, K. Takanabe, G. Xin, J. M. Carlsson, K. Domen and M. Antonietti, *Nat. Mater*. 2009, **8**, 76-80.
2 J. Liu, Y. Liu, N. Y. Liu, Y. Z. Han, X. Zhang, H. Huang, Y. Lifshitz, S.-T. Lee, J. Zhong and Z. H. Kang, *Science* 2015, **347**, 970-974.
3 V. W. H. Lau, M. B. Mesch, V. Duppel, V. Blum, J. Senker and B. V. Lotsch, *J. Am. Chem. Soc.* 2015, **137**, 1064-1072.
4 D. J. Martin, K. P. Qiu, S. A. Shevlin, A. D. Handoko, X. W. Chen, Z. X. Guo and J. W. Tang, *Angew. Chem. Int. Ed.* 2014, **53**, 9240 –9245.
5 S. W. Cao, J. X. Low, J. G. Yu and M. Jaroniec, *Adv. Mater.* 2015, **27**, 2150-2176.
6 J. Mao, T. Y. Peng, X. H. Zhang, K. Li, L. Q. Ye and L. Zan, *Catal. Sci. Technol*. 2013, **3**, 1253-1260.
7 Y. Li, H. Zhang, P. Liu, D. Wang, Y. Li and H. Zhao, *Small* 2013, **9**, 3336-3344.
8 P. Niu, L. L. Zhang, G. Liu and H. M. Cheng, *Adv. Funct. Mater.* 2012, **22**, 4763-4770.
9 X. D. Zhang, X. Xie, H. Wang, J. J. Zhang, B. C. Pan and Y. Xie, *J. Am. Chem. Soc.* 2013, **135**, 18-21.
10 T. Y. Ma, Y. H. Tang, S. Dai and S. Z. Qiao, *Small* 2014, **10**, 2382-2389.
11 J. Xu, L. W. Zhang, R. Shi and Y. F. Zhu, *J. Mater. Chem. A* 2013, **1**, 14766-14772.
12 K. Schwinghammer, M. B. Mesch, V. Duppel, C. Ziegler, J. Senker and B. V. Lotsch, *J. Am. Chem. Soc.* 2014, **136**, 1730-1733.
13 F. X. Cheng, H. N. Wang, X. P. Dong, *Chem. Commun.* 2015, **51**, 7176-7179.
14 Y. Xiao, L. Y. Zeng, T. Xia, Z. J. Wu and Z. H. Liu, *Angew. Chem. Int. Ed.* 2015, **54**, 5323-5327.
15 Z. Li, S. W. Lv, Y. L. Wang, S. Y. Chen and Z. H. Liu, *J. Am. Chem. Soc.* 2015, **137**, 3421-3427.
16 J. S. Zhang, G. G. Zhang, X. F. Chen, S. Lin, L. Mohlmann, G. Dolega, G. Lipner, M. Antonietti, S. Blechert and X. C. Wang, *Angew. Chem. Int. Ed.* 2012, **51**, 3183-3187.
17 J. Q. Tian, Q. Liu, A. M. Asiri, A. O. Al-Youbi and X. P. Sun, *Anal. Chem*. 2013, **85**, 5595-5599.
18 S. B. Yang, Y. J. Gong, J. S. Zhang, L. Zhan, L. L. Ma, Z. Y. Fang, R. Vajtai, X. C. Wang and P. M. Ajayan, *Adv. Mater.* 2013, **25** 2452-2456.
19 J. S. Zhang, M. W. Zhang, S. Lin, X. Z. Fu and X. C. Wang, *J. Catal*. 2014, **310**, 24-30.
20 Y. N. Tang, W. H. Di, X. S. Zhai, R. Y. Yang and W. P. Qin, *ACS Catal*. 2013, **3**, 405-412.
21 X. Y. Guo, W. Y. Song, C. F. Chen, W. H. Di and W. P. Qin, *Phys. Chem. Chem. Phys*. 2013, **15**, 14681-14688.
22 W. Wang, M. Y. Ding, C. H. Lu, Y. R. Ni and Z. Z. Wu, *Appl. Catal. B-Environ.* 2014, **144**, 379-385.
23 W. K. Su, M. M. Zheng, L. Li, K. Wang, R. Qiao, Y. J. Zhong, Y. Hu and Z. Q. Li, *J. Mater. Chem. A* 2014, **2**, 13486-13491.
24 Y. H. Zhang, L. X. Zhang, R. R. Deng, J. Tian, Y. Zong, D. Y. Jiang and X. G. Liu, *J. Am. Chem. Soc.* 2014, **136**, 4893-4896.
25 J. J. Peng, W. Xu, C. L. Teoh, S. Y. Han, B. Kim, A. Samanta, J. C. Er, L. Wang, L. Yuan, X. G. Liu and Y. T. Chang, *J. Am. Chem. Soc.* 2015, **137**, 2336-2342.
26 J. Y. Zhang, Y. H. Wang, J. Jin, J. Zhang, Z. Lin, F. Huang and J. G. Yu, *ACS Appl. Mater. Inter*. 2013, **5**, 10317-10324.
27 J. S. Xu, T. J. K. Brenner, Z. P. Chen, D. Neher, M. Antonietti and M. Shalom, *ACS Appl. Mater. Inter*. 2014, **6**, 16481-16486.